Cored dark-matter profiles in z≃1 star forming galaxies

Bouché, N.F.; Bera, S.; Krajnović, D.; Emsellem, E.; Mercier, W.; Schaye, J.; ... ; Venot, O.

SF2A 2021
A. Siebert, K. Baillié, E. Lagadec, N. Lagarde, J. Malzac, J.-B. Marquette, M. N'Diaye, J. Richard, O. Venot (eds)

CORED DARK-MATTER PROFILES IN $Z \simeq 1$ STAR FORMING GALAXIES

N. F. Bouché [1], S. Bera[1], D. Krajnović[2], E. Emsellem[3], W. Mercier[4], J. Schaye[5], B. Epinat[6], J. Richard[1], S. L. Zoutendijk[5], V. Abril-Melgarejo[6], J. Brinchmann[7], R. Bacon[1], T. Contini[4], L. Boogaard[5 8], L. Wisotzki[2], M. Maseda[6] and M. Steinmetz[2]

Abstract. We present a study of the dark-matter (DM) content of 9 $z \approx 1$ low mass SFGs (with $M_\star$ ranging from $10^{8.5}$ to $10^{10.5}$ $M_\odot$) selected among the brightest [O II] emitters in the deepest Multi-Unit Spectrograph Explorer (MUSE) field to date, namely the 140hr MUSE Extremely Deep Field. We perform disk-halo decompositions on their [O II] emission line with a 3D parametric model using GalPaK^{3D}. The disk-halo decomposition includes a stellar, DM, gas and occasionally a bulge component, and the DM component is made of a generalized α, β, γ profile. We find that the disk stellar masses $M_\star$ obtained from the [O II] disk-halo decomposition agree with the values inferred from the spectral energy distributions. We find that the rotation curves show diverse shapes, ranging from rising to declining at large radii, the DM fractions within the half-light radius $f_{\rm DM}(< R_{\rm e})$ are found to be 60% to 95%, extending to lower masses (densities) the results of Genzel et al. For isolated galaxies, same SFGs shows a strong preference for cored over cuspy DM profiles and the presence of DM cores occurs in galaxies with low stellar-to-halo mass ratio, $\log M_\star/M_{\rm vir} \approx -2.5$. The cored/cuspiness nature of the DM profiles is found to be a strong function of the recent star-formation activity, supporting feedback induced core formation in the Cold Dark Matter context.

Keywords: galaxies: evolution; galaxies: high-redshift; galaxies: kinematics and dynamics; methods: data analysis

1 Introduction

The universe's matter content is dominated by the elusive dark-matter (DM), which has yet to be discovered and understanding the nature and properties of DM on galactic scales remains one of the greatest challenges of modern physics and cosmology (see Bullock & Boylan-Kolchin 2017, for a review). The concept of DM became part of mainstream research only in the 1970s, when it was realized that galaxy rotation curves (RCs) became flat at large radii (e.g. Rubin & Ford 1970), which could not be explained within the standard Newtonian gravity framework, but instead implied the presence of an unobserved mass component attributed to a DM halo.

Understanding the relative distributions of baryons and dark matter in galaxies is still best achieved from a careful analysis of galaxies' RCs on galactic scales. At redshift $z = 0$, this type of analysis is mature with a wealth of studies published in the past 20-30 years, using a variety of dynamics tracers such as H I (e.g. de Blok & McGaugh 1997; de Blok et al. 2001) or a combination of H I & Hα as in the recent SPARC sample (Allaert et al. 2017; Katz et al. 2017; Li et al. 2020). In low surface brightness (LSB) galaxies, the DM profiles have shown to be consistent with a flat density inner 'core', contrary to the expectations from DM-only simulations that

[1] Univ Lyon, Univ Lyon1, Ens de Lyon, CNRS, Centre de Recherche Astrophysique de Lyon (CRAL) UMR5574, F-69230 Saint-Genis-Laval, France
[2] Leibniz-Institut für Astrophysik Potsdam (AIP), An der Sternwarte 16, D-14482 Postdam, Germany
[3] ESO, Karl-Schwarzschild-Strasse 2., D-85748 Garching b. München, Germany
[4] Institut de Recherche en Astrophysique et Planétologie (IRAP), Université de Toulouse, CNRS, UPS, F-31400 Toulouse, France
[5] Leiden Observatory, Leiden University, P.O. Box 9513, 2300 RA Leiden, The Netherlands
[6] Aix Marseille Univ, CNRS, CNES, LAM, Marseille, France
[7] Instituto de Astrofísica e Ciências do Espaço, Universidade do Porto, CAUP, Rua das Estrelas, 4150-762 Porto, Portugal
[8] Max Planck Institute for Astronomy, Königstuhl 17, 69117 Heidelberg, Germany

predicts steep central density profiles or 'cusp' (e.g. Navarro et al. 1997, NFW). It has long been recongnized that this cusp-core debate can be resolved within CDM with feedback processes (e.g. Navarro et al. 1996; Pontzen & Governato 2012).

At high redshifts, where 21cm observations are not yet available, it is very difficult to measure the DM content of high-redshift galaxies from the kinematics in the outskirts of individual star-forming galaxies (SFGs) using nebular lines (e.g. Hα), because of the exponential decrease in signal-to-noise (S/N). But thanks to the pioneering work of Genzel et al. (2017), disk-halo decompositions have proven to be possible at $z \simeq 2$ using deep (> 30 hr) near-IR integral field spectroscopy (IFS) on a small sample of six massive star-forming galaxies (SFGs) (see also Genzel et al. 2020; Rizzo et al. 2021).

Here, we perform a disk-halo decomposition in *individual* low-mass SFGs at intermediate redshifts ($0.6 < z < 1.1$) using the deepest (140hr) Multi-Unit Spectroscopic Explorer (MUSE Bacon et al. 2010) data obtained on the *Hubble* Ultra Deep Field (HUDF Bacon et al. 2021) and 3D algorithms such as GalPaK^{3D} (Bouché et al. 2015). Tthanks to the combination of 3D modeling approach and these extremely deep IFU data, rotation curves can be constrained up to 3 R_e in individual galaxies.

2 Data and Methodology

2.1 Sample

From the recent MUSE eXtremely Deep Field (MXDF) region of the HUDF (Bacon et al. 2021) We selected 9 [O II] emitters with the highest S/N per spaxel in [O II], with pixel S/N reaching $S/N_{pix} \sim 100$ in the central spaxel. These galaxies have redshifts ranging from 0.6 to 1.1, and have stellar masses from $M_\star = 10^{8.9}$ $M_\odot$ to $M_\star = 10^{10.3}$ $M_\odot$ with SFRs from 1 to 5 $M_\odot$ yr^{-1}. The stellar masses and SFR were determined from spectral energy distribution (SED) fits with the Magphys (da Cunha et al. 2015) software on the HST photometry.

2.2 Method

In order to measure individual RCs in the outskirts of individual SFGs, at radii up to 10-15 kpc (2-3 Re) where the S/N per spaxel falls below unity, we use the GalPaK^{3D} algorithm (Bouché et al. 2015) which compares 3D parametric models directly to the 3D data, taking into account the instrumental resolution and PSF*. Note this 3D algorithm GalPaK^{3D} allows to fit the kinematics and morphological parameters *simultaneously* and thus no prior information is required on the inclination †. The agreement between HST-based and MUSE-based inclinations is typically better than 7°(rms) for galaxies with $25 < i < 80$ as demonstrated in Contini et al. (2016) and with mock data-cubes (Bouché et al. 2021) derived from the Illustris "NewGeneration 50 Mpc" (TNG50) simulations.

For the morphology, the model assumes a Sérsic (1963) surface brightness profile $\Sigma(r)$, with Sérsic index n. The disk model is inclined to any given inclination i and orientation or positional angle (P.A). The thickness profile is taken to be Gaussian whose scale height h_z is $0.15 \times R_e$. For [O II] emitters, as in this analysis, we add a global [O II] doublet ratio r_{O2}.

For the kinematics, the velocity dispersion profile $\sigma_t(r)$ consists of the combination of a thick disk σ_{thick}, defined from the identity $\sigma_{thick}(r)/v(r) = h_z/r$ (Genzel et al. 2006; Cresci et al. 2009) where h_z is the disk thickness (taken to be $0.15 \times R_e$) and a dispersion floor, σ_0, added in quadrature (similar to σ_0 in Genzel et al. 2006, 2008).

We perform a disk-halo decomposition of the rotation curve $v(r)$ into the following components

$$v_c^2(r) = v_{dm}^2(r) + v_d^2(r) + v_g^2(r), \tag{2.1}$$

where v_{dm} is the DM component, v_d the disk component (stellar and molecular) and an atomic a gas v_g component. The mass profile in molecular gas and star are inherently degenerate without direct CO measurements, but given that the molecular gas fractions are typically 30-50% (e.g. Tacconi et al. 2018; Freundlich et al. 2019), this amounts to a systematic uncertainty of 0.1-0.15 dex on the disk component. The disk component v_d is modelled as a Freeman (1970) disk suitable for exponential mass profiles and most of our galaxies have stellar Sérsic indices $n_\star$ close to $n_\star \simeq 1$.

*See `http://galpak3d.univ-lyon1.fr`.

†The traditional $i - V_{max}$ degeneracy is broken using the morphological information, specifically the axis b/a ratio.

The DM component $v_{\rm dm}(r)$ is modelled as a Hernquist-Zhao profile following Di Cintio et al. (2014, hereafter DC14):

$$\rho(r;\rho_s,r_s,\alpha,\beta,\gamma) = \frac{\rho_s}{\left(\frac{r}{r_s}\right)^{\gamma}\left(1+\left(\frac{r}{r_s}\right)^{\alpha}\right)^{(\beta-\gamma)/\alpha}} \tag{2.2}$$

where r_s is the scale radius, ρ_s the scale density, and α, β, γ are the shape parameters, with β corresponding to the outer slope, γ the inner slope and α the transition sharpness. In simulations with supernova feedback (e.g. DC14, Tollet et al. 2016; Lazar et al. 2020), the shape parameters α, β, γ in Eq. 2.2 are a direct function of the disk-to-halo mass ratio $\log X \equiv \log(M_\star/M_{\rm vir})$. Here, we used the $\alpha(X), \beta(X), \gamma(X)$ parametrisation with $\log M_\star/M_{\rm vir}$ from DC14 (their Eq.3), and this DM profile $v_{\rm dm}(r)$ has three free parameters, namely $\log X, V_{\rm vir}$ and the concentration c_{-2} defined as $c_{{\rm vir},-2} \equiv R_{\rm vir}/r_{-2}$, where $R_{\rm vir}$ is the halo virial radius.

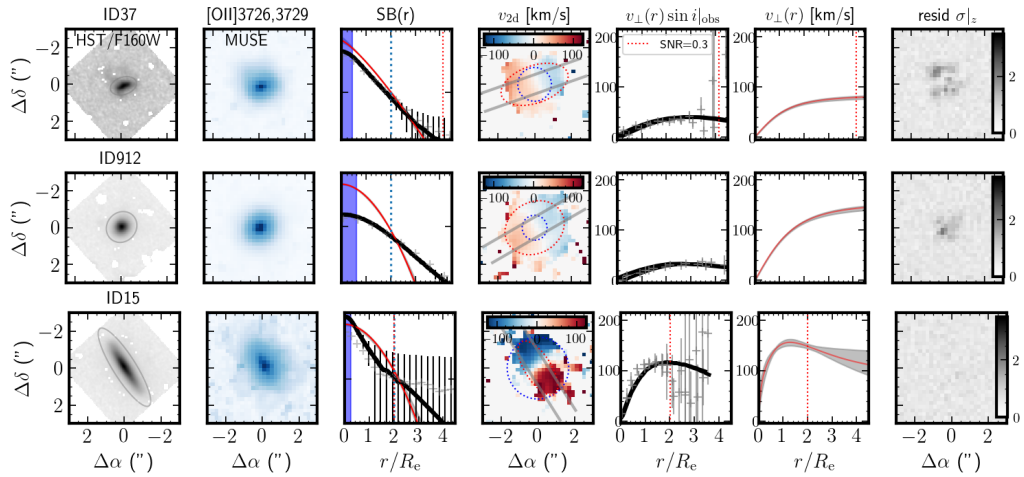

Fig. 1. Examples of 3D morpho-kinematics modelling. Each panel show the stellar continuum from *HST*/F160W, the [O II] flux map from MUSE, the [O II] surface brightness profile (SB(r)), the observed projected velocity field (v_{2d}), the observed 1d velocity profile $v_\perp \sin i$, the intrinsic (i.e. deprojected, corrected for beam smearing) modeled rotation curve ($v_\perp$) using the model of (Persic et al. 1996).

3 Results

We find that the 3D approach allows to constrain RCs to $3R_{\rm e}$ in individual SFGs revealing a diversity in shapes with mostly rising and some having declining outer profiles (Fig. 1). The disk stellar mass $M_\star$ from the [O II] rotation curves is consistent with the SED-derived $M_\star$, except for two SFGs whose kinematics are strongly perturbed by a nearby companion (< 2"). With this sample of SFGs which have stellar masses (from $10^{8.5}{\rm M}_\odot$ to $10^{10.5}{\rm M}_\odot$), the DM fractions $f_{\rm DM}(< R_{\rm e})$ are high (60-90%) (Fig. 2a). These DM fractions complement the low fractions of the sample of Genzel et al. (2020), and globally, the $f_{\rm DM}(< R_{\rm e}) - \Sigma_\star$ relation is similar to the $z = 0$ relation (e.g. Courteau & Dutton 2015), and follows from the TFR. We wind that the DM concentrations are consistent with the $c_{\rm vir} - M_{\rm vir}$ scaling relation predicted by DM only simulations. Finally, DM cores are present in galaxies with high SFRs (Fig. 2b), supporting the scenario of SN feedback-induced core formation.

This study is based on observations collected at the European Southern Observatory under ESO programme 1101.A-0127. This work has been carried out in part thanks to the support of the ANR 3DGasFlows (ANR-17-CE31-0017), the OCEVU Labex (ANR-11-LABX-0060), the Programme National Cosmology et Galaxies (PNCG) of CNRS/INSU with INP and IN2P3, co-funded by CEA and CNES. R.B. acknowledges support from the ERC advanced grant 339659-MUSICOS.

References

Allaert, F., Gentile, G., & Baes, M. 2017, A&A, 605, A55

Bacon, R., Accardo, M., Adjali, L., et al. 2010, in Society of Photo-Optical Instrumentation Engineers (SPIE) Conference Series, Vol. 7735, Society of Photo-Optical Instrumentation Engineers (SPIE) Conference Series, 8

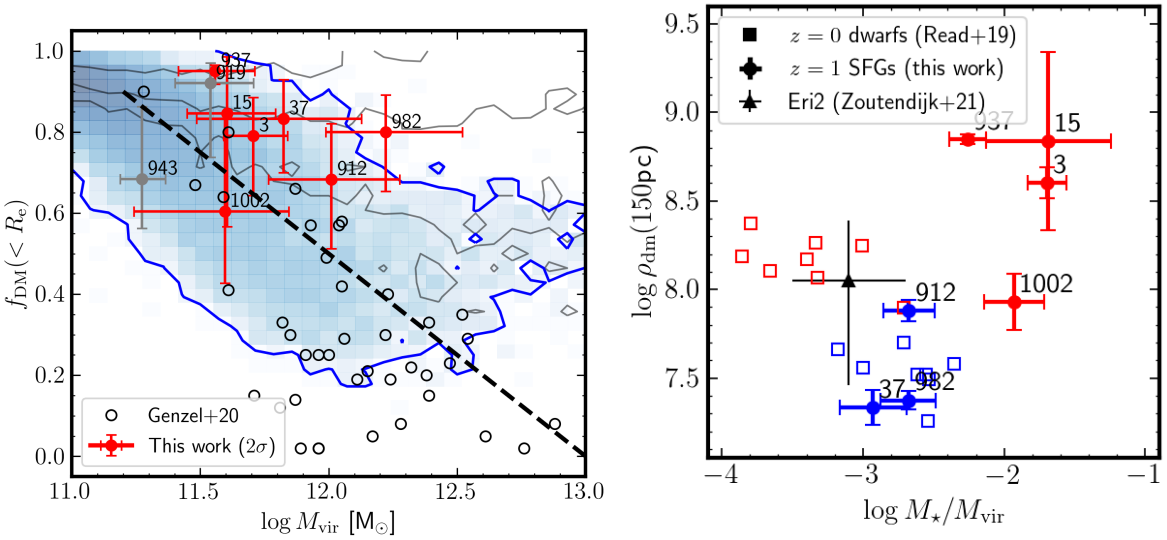

Fig. 2. Left: The DM fractions within the half-light radius $R_{\rm e}$, $f_{\rm DM}(< R_{\rm e})$, as a function of halo mass, $M_{\rm vir}$. The dashed line represent the downwards trend of Genzel et al. (2020). **Right:** The DM density at 150pc as a function of $\log M_\star/M_{\rm vir}$. The blue (red) solid circles with error bars (2σ) represent our SFGs with high (low) $\Sigma_{\rm SFR}$, respectively. The blue (red) open squares represent the $z \approx 0$ dwarfs from Read et al. (2019) whose SFR was truncated less (more) than 6 Gyrs ago.

Bacon, R., Mary, D., Garel, T., et al. 2021, A&A, 647, A107
Bouché, N. F., Carfantan, H., Schroetter, I., Michel-Dansac, L., & Contini, T. 2015, AJ, 150, 92
Bouché, N. F., Genel, S., Pellissier, A., et al. 2021, A&A, in press (arXiv/2101.12250)
Bullock, J. S. & Boylan-Kolchin, M. 2017, ARA&A, 55, 343
Contini, T., Epinat, B., Bouché, N., et al. 2016, A&A, 591, A49
Courteau, S. & Dutton, A. A. 2015, ApJ, 801, L20
Cresci, G., Hicks, E. K. S., Genzel, R., et al. 2009, ApJ, 697, 115
da Cunha, E., Walter, F., Smail, I. R., et al. 2015, ApJ, 806, 110
de Blok, W. J. G. & McGaugh, S. S. 1997, MNRAS, 290, 533
de Blok, W. J. G., McGaugh, S. S., & Rubin, V. C. 2001, AJ, 122, 2396
Di Cintio, A., Brook, C. B., Dutton, A. a., et al. 2014, MNRAS, 441, 2986
Freeman, K. C. 1970, ApJ, 160, 811
Freundlich, J., Combes, F., Tacconi, L. J., et al. 2019, A&A, 622, A105
Genzel, R., Burkert, A., Bouché, N., et al. 2008, ApJ, 687, 59
Genzel, R., Price, S. H., Übler, H., et al. 2020, ApJ, 902, 98
Genzel, R., Schreiber, N. M. F., Übler, H., et al. 2017, Nature, 543, 397
Genzel, R., Tacconi, L. J., Eisenhauer, F., et al. 2006, Nature, 442, 786
Katz, H., Lelli, F., Mcgaugh, S. S., et al. 2017, MNRAS, 466, 1648
Lazar, A., Bullock, J. S., Boylan-Kolchin, M., et al. 2020, MNRAS, 497, 2393
Li, P., Lelli, F., McGaugh, S., & Schombert, J. 2020, ApJS, 247, 31
Navarro, J. F., Eke, V. R., & Frenk, C. S. 1996, MNRAS, 283, L72
Navarro, J. F., Frenk, C. S., & White, S. D. M. 1997, ApJ, 490, 493
Persic, M., Salucci, P., & Stel, F. 1996, MNRAS, 281, 27
Pontzen, A. & Governato, F. 2012, MNRAS, 421, 3464
Read, J. I., Walker, M. G., & Steger, P. 2019, MNRAS, 484, 1401
Rizzo, F., Vegetti, S., Fraternali, F., Stacey, H., & Powell, D. 2021, MNRAS
Rubin, V. C. & Ford, W. Kent, J. 1970, ApJ, 159, 379
Sérsic, J. L. 1963, BAAA, 6, 41
Tacconi, L. J., Genzel, R., Saintonge, A., et al. 2018, ApJ, 853, 179
Tollet, E., Macci, A. V., Dutton, A. A., et al. 2016, MNRAS, 456, 3542